




Article

On the Relationship between a Novel *Prorocentrum* sp. and Colonial *Phaeocystis antarctica* under Iron and Vitamin B₁₂ Limitation: Ecological Implications for Antarctic Waters

Francesco Bolinesi ¹, Maria Saggiomo ², Serena Aceto ¹ , Angelina Cordone ¹,
Emanuela Serino ³, Maria Carmen Valoroso ¹  and Olga Mangoni ^{1,3,*} 

¹ Dipartimento di Biologia, Università degli Studi di Napoli Federico II, Via Cinthia 21, 80126 Napoli, Italy; francesco.bolinesi@unina.it (F.B.); serena.aceto@unina.it (S.A.); angelina.cordone@unina.it (A.C.); mariacarmen.valoroso@unina.it (M.C.V.)

² Stazione Zoologica Anton Dohrn, Villa Comunale, 80121 Napoli, Italy; m.saggio@szn.it

³ CoNISMa, Piazzale Flaminio, 9, 00196 Roma, Italy; elamanu88@gmail.com

* Correspondence: olga.mangoni@unina.it; Tel.: +39-0812535132

Received: 28 August 2020; Accepted: 30 September 2020; Published: 5 October 2020



Featured Application: Since preliminary data revealed that *Prorocentrum* sp. (Dinophyceae) was able to produce bioactive compounds, further investigation will be focused on the isolation and identification of molecules potentially usable for biotechnological and pharmaceutical applications.

Abstract: We collected live mixed natural samples from the northeastern Ross Sea during the austral summer of 2017 and isolated a novel *Prorocentrum* sp. (Dinophyceae) associated with mucilaginous *Phaeocystis antarctica* (Coccolithophyceae) colonies. The haptophyte *P. antarctica* is a key species of the phytoplankton community in the Ross Sea, where blooms are subjected to iron limitation and/or co-limitation with other micronutrients (e.g., vitamin B₁₂) during the summer. We first performed preliminary genetic analyses to determine the specific identity of the novel *Prorocentrum* sp., which indicated that it represented a previously undescribed species. The formal description of this new species is in process. To further assess its relationship with *P. antarctica*, we obtained their monospecific and mixed cultures and evaluated their responses to different irradiance levels and iron and vitamin B₁₂ limitation. Our results indicated differential susceptibility of the two species to iron limitation and differential photosynthetic plasticity under high irradiance. Iron limitation reduced colony formation in *P. antarctica* and decreased the chlorophyll-a content in *Prorocentrum* sp., whereas B₁₂ limitation did not affect growth or photosynthetic efficiency in either species. In addition, *P. antarctica* could photosynthesize efficiently under different irradiance levels, due to its ability to modulate the light adsorption cross-section of PSII, whereas *Prorocentrum* sp. exhibited lower photosynthetic plasticity and an inability to modulate both the maximum photochemical efficiency and effective adsorption cross-section of PSII under high irradiance. The trophic interaction between *Prorocentrum* sp. and *P. antarctica* could present ecological implications for the food webs and biogeochemical cycles of the Antarctic ecosystem. Considering the predicted climate-driven shifts in global ocean surface light regimes and changes in iron or vitamin B₁₂ transfer, which are most likely to impact changes in the phytoplankton community structure, our results present implications for carbon export to deeper waters, ecological functioning, and associated biogeochemical changes in the future.

Keywords: Ross Sea; phytoplankton diversity; photosynthetic efficiency; climate change

1. Introduction

The Ross Sea is regarded to be the most productive area of the Southern Ocean, playing a key role in the transfer of atmospheric carbon to the ocean's interior and in global climate regulation [1,2]. The high productivity of this region is linked essentially to its phytoplankton community, which is dominated primarily by various diatoms (Bacillariophyceae) and the coccolithophyte *Phaeocystis antarctica*. These two functional groups exhibit different temporal and spatial patterns, with *P. antarctica* dominating the early seasonal blooms in the polynyas [2–5], accounting for more than 60% of the primary productivity in the southern Ross Sea [6], whereas diatoms dominate the coastal waters and the shallow upper mixed layer during the summer. Although the drivers regulating these blooms have been extensively investigated, the spatial and temporal differences between diatoms and *P. antarctica* present several avenues for further research [7,8]. Studies conducted in the last decade have demonstrated that these blooms were subject to seasonal iron limitation and/or co-limitation with other micronutrients (such as vitamin B₁₂) which could potentially influence the phytoplankton community structure [9–13]. The dominance of *P. antarctica* in early spring blooms has been attributed to its ability to photosynthesize efficiently under relatively low light levels [14–17] and to its remarkable tolerance to low iron concentrations as compared with the diatoms [18]. *P. antarctica* usually occurs in colonies during the blooming phase [19–21], with cells embedded in a thin mucous matrix forming a balloon-like colony, which can measure several hundred micrometers in diameter. This has been suggested to be a defense mechanism against grazers [22] such as *Euphausia superba* and, in turn, represents one of the most important prey items for several predators in the Antarctic waters. In the case of other less abundant groups, an increase in dinoflagellates, silicoflagellates, and heterotrophic protists has been reported in the phytoplankton communities later in the growing season [23–26]. The first detailed research on Southern Ocean dinoflagellates was started by Balech [27] who identified different species in 1976 [28], and the group has been later reported during both spring and summer in the Ross Sea (<http://www.bco-dmo.org/dataset/2732> and <http://www.bco-dmo.org/dataset/3360>). Some dinoflagellates described in the Ross Sea are capable of kleptoplastidy [29] and have been noted within *P. antarctica* colonies, although the *P. antarctica* morphotype that serves as the plastid source remains unknown [30,31]. Drivers regulating phytoplankton blooms in the Ross Sea have received significant attention in the last decade, which has led to several studies being conducted and new discoveries being made, including a new species of dinoflagellates belonging to the genus *Protoperdinium* that was recently described by Phan-Tan [31] in the south-central Ross Sea. Because the dominance of different functional groups channels the energy flow through different trophic patterns, thus, differentially influencing the export of carbon aggregates out of the photic zone [32,33], the discovery of new phytoplankton species could reflect the changes occurring in the Antarctic waters, inciting the re-evaluation of the role of minor functional groups within the phytoplankton community of the Ross Sea. In the present study, we isolated a new dinoflagellate species belonging to the genus *Prorocentrum* from colonial *P. antarctica* collected from the central Ross Sea, and defined its growth rate and photophysiological responses to varying light intensities, as well as iron and vitamin B₁₂ limitation, in both monospecific and mixed cultures with *P. antarctica*.

2. Materials and Methods

2.1. Phytoplankton Collection, Isolation, and Culture

Seawater samples were collected during the austral summer of 2017 onboard the R/V *Italica*, using a rosette sampler equipped with Niskin bottles, under the P-ROSE Project (Plankton biodiversity and functioning of the Ross Sea ecosystems in a changing Southern Ocean-XXXII Italian Antarctic Expedition). At each station, 30 mL of sea water was withdrawn from the Niskin bottles, prefiltered through a 300 µm mesh (Nitexs, Wildlife Supply Company, Buffalo, NY, USA) to remove most metazoan plankton, and inoculated in 60 mL flasks filled with sterilized Ross Sea water enriched with 20% L1 medium. After inoculation, the flasks were incubated at 3 °C under continuous light at an intensity

of $\sim 40 \mu\text{mol photons m}^{-2} \text{s}^{-1}$. All samples were checked periodically using a light microscope and refreshed every 2 weeks until the end of the cruise. On reaching Italy, the incubator with the live mixed samples was transported from the R/V *Italica* to the laboratory of Marine Ecology at the University of Naples Federico II. All flasks were refrigerated at $1.5 \text{ }^\circ\text{C}$ under continuous light at $\sim 40 \mu\text{mol photons m}^{-2} \text{s}^{-1}$ and refreshed using 50% L1 medium with a salinity of 34, generating a series of replicates for each sample.

After acclimatization for 2 weeks, individual phytoplankton species were isolated to prepare monospecific cultures. Phytoplankton were isolated by Francesco Bolinesi, following the procedure suggested by C. R. Tomas, of the Center for Marine Science, University of North Carolina, Wilmington, USA (personal communication), and involved both serial dilution and single cell collection using handheld micropipettes and an inverted light microscope (Leica DMIL led).

Considering the isolation of *P. antarctica*, single balloon-like colonies were collected using a modified micropipette and transferred to a 96-well rack in sterile conditions under a laminar hood (ASALAIR 700), until one colony per well was obtained. Each well was filled with 0.3 mL of seawater enriched with 50% L1 medium. Once cells started to replicate, we transferred three colonies to a 24-well rack, and after two weeks, when cells achieved the maximum growth rate, $\sim 2 \text{ mL}$ of the sample from each well were inoculated in 60 mL flasks, and new medium was added at 50% volume of the sample. Flasks were periodically checked using a Phyto-PAM Compact Unit (Walz) to evaluate photosynthetic quantum efficiency, and samples were subjected to high performance liquid chromatography (HPLC) to determine the pigment spectral composition and to identify the marker pigment of each isolated species [34–36]. By doing this, a signal corresponding to Peridinin (Perid), the marker pigment of dinoflagellates, was detected in colonial *P. antarctica* cultures, especially under nutrient starvation. Thorough microscopic examination of the culture yielded a previously unknown species of dinoflagellate, resembling *Prorocentrum minimum* (Dinophyceae), associated with the mucilaginous sheath of *P. antarctica* colonies. This unknown dinoflagellate species was isolated using a modified micropipette, breaking colonies mechanically, and the first monospecific culture was obtained after culturing for eight weeks, and then subjected to HPLC to obtain the pigment spectra. The isolates were cultured under standard growth conditions of $1.5 \text{ }^\circ\text{C}$, 100% L1 medium, and continuous light at $40 \mu\text{mol photons m}^{-2} \text{s}^{-1}$ (Figure 1). The pigment spectra of the two species are reported in Figure 2.

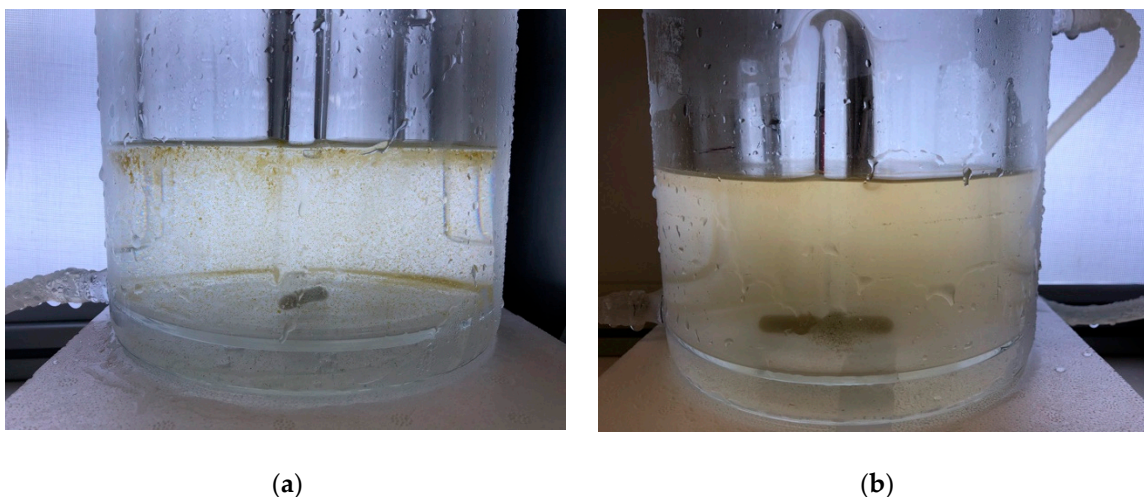


Figure 1. (a) *Phaeocystis antarctica*; (b) *Prorocentrum* sp.

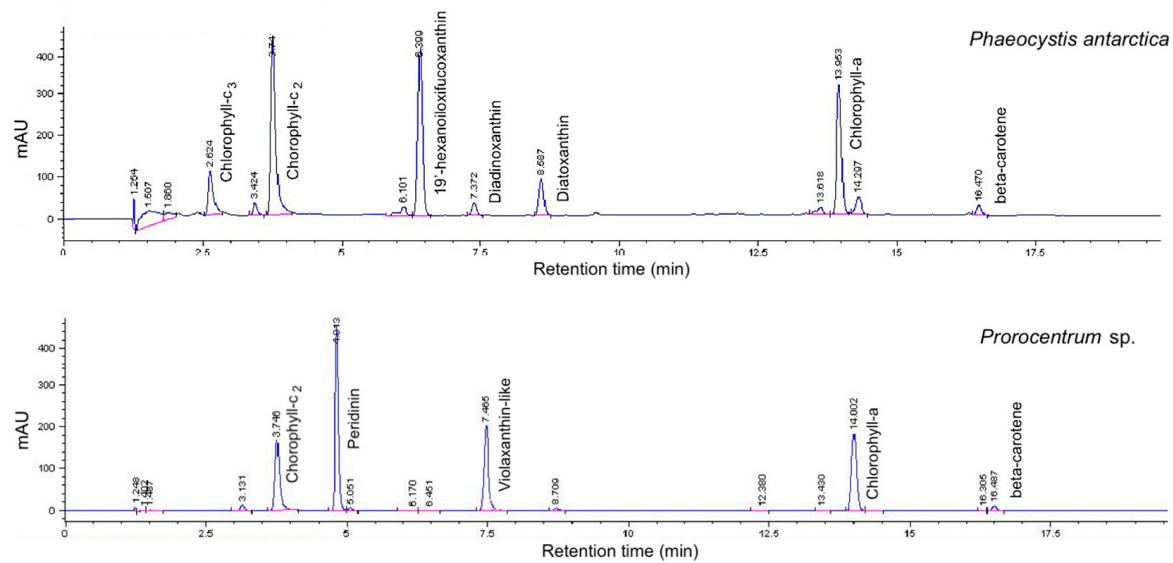


Figure 2. Chromatograms in absorbance (mAU) of the two species.

2.2. Molecular Analysis and Identification of the Two Species

Total DNA was extracted from the monospecific cultures of *P. antarctica* and the associated unknown dinoflagellate by the CTAB method [37].

Regions of the small (18S) and large (28S) ribosomal RNA genes of *P. antarctica* were amplified by PCR, using the primer pairs 18SF2/18SR2 (5'-AGGGCAAGTCTGGTGCCAG-3' and 5'-CCTTCCGCAGGTTACCTAC-3') and 28SF/28SR (5'-CCGCTGAATTTAAGCATAT-3' and 5'-CTTGGTCCGTGTTTCAAGAC-3') [38].

Regions of the ribosomal RNA cluster genes, from the small (18S) to the large (28S) subunit genes and including ITS1, 5.8S gene, and ITS2, of the unknown dinoflagellate were amplified by PCR, using the primer pairs DR1/LSUB (5'-ACCCGCTGAATTTAAGCATA-3' and 5'-ACGAACGATTTGCACGTCAG-3') for the large subunit (LSU) [39,40], SR4/SR12 (5'-AGGGCAAGTCTGGTGCCAG-3' and 5'-CCTTCCGCAGGTTACCTAC-3') and SR1/SR5TAK (5'-TACCTGGTTGATCCTGCCAG-3' and 5'-ACTACGAGCTTTTAAACYGC-3') [41] for the small subunit (SSU), and JK14/25R1 [42,43] for the region from ITS1 to LSU encompassing the 5.8S gene and ITS2.

Amplification was performed in a final reaction volume of 50 μ L, containing 10 ng of DNA, 0.3 μ M of each primer, 200 μ M of dNTPs, and 1 U XtraTaq Pol White (Genespin) in 1X reaction buffer. The cycling conditions were as follows: initial denaturation at 95 $^{\circ}$ C for 1 min; 35 cycles of 95 $^{\circ}$ C for 30 s, 52 $^{\circ}$ C for 30 s, and 72 $^{\circ}$ C for 1 min; and final elongation at 72 $^{\circ}$ C for 10 min. The amplification products were cloned into the pSC-A-amp/kan vector (Agilent) and sequenced using specific primers (Eurofins Genomics). The obtained sequences were analyzed using BLASTn, and then deposited in GenBank with the accession numbers MT831989 and MT831990 for the small and large ribosomal gene fragments of *P. antarctica*, respectively, and MT830911 and MT831988 for the small and ITS-5.8S large ribosomal gene fragments of the *Prorocentrum* sp., respectively.

2.3. Experimental Setup

2.3.1. Experiment 1: Iron and B₁₂ Limitation

To study the growth rate and photophysiological responses of *Prorocentrum* sp. and *Phaeocystis antarctica* under iron and vitamin B₁₂ limitation in monospecific and mixed cultures, we performed an experiment including three different growth conditions, i.e., 100% L1 medium without iron (i.e., with added desferoxamine B (DFB), Sigma-Aldrich), 100% L1 medium without vitamin B₁₂ (-B₁₂) Sigma-Aldrich, and 100% L1 medium as the control (CTRL) as follows:

1. For the DFB treatment, we prepared L1 medium without iron (II). As natural oligotrophic seawater was used as a base for the medium, we added DFB as a ligand to chelate all dissolved iron, to achieve a final DFB/iron (II) ratio of 100:1, assuming an iron concentration of 5 nM.
2. For the -B12 treatment, modified 100% L1 medium was prepared by excluding vitamin B₁₂ from the vitamin stock solution. The amount of vitamin B₁₂ present in the prefiltered (0.2 µm mesh size) seawater used as the culture medium before the addition of L1 medium would be negligible as seawater samples were sterilized by autoclaving at 1.06 kg cm⁻² for 20 min.
3. For the CTRL treatment (i.e., with both iron and B₁₂) 100% L1 medium was used.

The flasks used for incubating the samples were soaked overnight in 1% citranox (Alconox) to remove trace metals, rinsed six times with Milli-Q water, soaked in 10% HC1 (Baker Instra-analyzed) for at least 3 days, and then rinsed three times with Milli-Q water (Ph = 2) prior to use. Flasks were prepared in a positive-pressure trace metal clean area using established trace metal clean techniques for incubation.

The two species were grown in flasks under continuous light at 40 µmol photons m⁻² s⁻¹, in 100% L1 medium at 1.5 °C, until the maximum growth rate was achieved. In the case of *Prorocentrum* sp., 20 mL of the isolates were inoculated in 250 mL flasks containing the appropriate medium for one of the three treatments. All treatments were performed in triplicate, yielding a total of 27 flasks for the entire experiment, i.e., 9 flasks for each culture and 3 cultures. *P. antarctica* were cultured following the same procedure. For the mixed cultures, flasks were inoculated with 10 mL each of *Prorocentrum* sp. and *P. antarctica*. At the beginning of the experiment, the pigment spectral composition, photosynthetic efficiency, total biomass, and total cell count of the cultures were determined using HPLC, Phyto-PAM, spectrofluorometric analysis of the chlorophyll-a (Chl-a) content, and Bürker counting chamber, respectively.

Single time point sampling was performed daily at the same time for 16 days, for evaluating the maximum PSII photochemical efficiency (Fv/Fm), the maximum PSII effective absorption cross-section (σPSII), and Chl-a content. At the end of the experiment, i.e., after 16 days, the pigment spectral composition of each treatment was obtained using HPLC, and the total cell count was determined to calculate the Chl-a/cell ratio for *Prorocentrum* sp. and *P. antarctica*.

2.3.2. Experiment 2: Exposure to Varying Light Intensity

The photophysiological responses of *P. antarctica* and *Prorocentrum* sp. under nonlimiting nutrient concentrations were assessed at four levels of light intensity, as follows: high light (HL), 220 mmol photons m⁻² s⁻¹; low light 1 (L1), 90 mmol photons m⁻² s⁻¹; low light 2 (L2), 60 mmol photons m⁻² s⁻¹; and low light 3 (L3), 25 mmol photons m⁻² s⁻¹. The light inside the culture flasks was measured using a spherical sensor (QSL-100, Biospherical Instruments Inc.) and neutral density screens were used to modulate the light intensity. The cultures were grown in TPP (Techno Plastic Products, Cole-Palmer) flasks containing 100% L1 medium, prepared following [44], at 4 °C, and the suspension was maintained by daily shaking. Twenty-four 250 mL flasks were prepared in total for the experiment.

2.4. Pigment Analysis

For evaluating the total Chl-a content, 10 mL of the culture was filtered through Whatman GF/F filters (25 mm diameter). Chl-a and phaeopigments (Phaeo) were analyzed following [45], using a Shimadzu spectrofluorometer, which was calibrated and checked daily using a standard Chl-a solution (*Anacystis nidulans*, Cyanophyceae, Sigma).

To determine accessory pigments by HPLC, 40 mL of the culture was filtered using Whatman GF/F filters (47 mm diameter) and stored at -80 °C until pigment analysis. Pigments were separated on an Agilent 1100 HPLC system, following the method described by [46] with modifications suggested by [47]. The system was equipped with an HP 1050 photodiode array detector and an HP 1046A fluorescence detector for the determination of chlorophyll degradation products. Instruments were calibrated using

20 different pigment standards provided by the International Agency for ^{14}C Determination, VKI Water Quality Institute, Copenhagen, Denmark. The marker pigments used to identify the contribution of the major phytoplankton taxa were 19'-hexanoyloxyfucoxanthin (Hex) and chlorophyll-c₃ (Chl-c₃) for *Phaeocystis antarctica* and peridinin (Perid) for *Prorocentrum* sp. [48–51].

The carotenoids involved in photoregulatory processes through the xanthophyll cycle were analyzed following previously described methods [52–54]. The photoprotective pigment ratio was calculated as the ratio of the sum of diadinoxanthin (Dd) and diatoxanthin (Dt) to Chl-a ($(\text{Dd} + \text{Dt})/\text{Chl-a}$). The de-epoxidation state of the xanthophyll cycle was expressed as the ratio of Dt to Dd + Dt ($\text{Dt}/(\text{Dd} + \text{Dt})$).

2.5. Photosynthetic Efficiency

The Fv/Fm and σPSII , which describe the functional “target area” of the light harvesting antenna that is energetically coupled to the O₂-releasing reaction centers (RCIIIs) [55,56], were determined using a Phyto_PAM II compact unit (Walz). All samples were acclimatized for 30 min in the dark before analysis to minimize the non-photochemical dissipation of excitation, and measurements were blank corrected by filtering the sample through a 0.2 μm filter [57]. For determining Fv/Fm, samples were illuminated with a saturating pulse following [58], and the ratio was calculated using the formula $\text{Fv/Fm} = (\text{Fm} - \text{F0})/\text{Fm}$. For determining σPSII at 440 nm, we used the fast kinetics windows (Phyto Win_3 software) to analyze the wavelength dependent O-I1 fluorescence rise kinetics under pulses of strong actinic light. The PAR-List was calibrated using a spherical micro quantum sensor (US-SQS/WB) prior to analysis. All samples were far-red pre-illuminated before analysis to inhibit the PSI response [59].

3. Results

3.1. Identification of a Novel *Prorocentrum* sp. from *Phaeocystis* Antarctica Colonies

The BLASTn analysis revealed that the sequenced fragment of the small ribosomal subunit (1698 bp) of the unknown dinoflagellate shared the highest nucleotide identity with *Prorocentrum minimum* (99.5%). However, the sequenced fragment including the ITS1, 5.8S gene, the ITS2, and the large ribosomal subunit (1508 bp) fragment shared only 94.75% identity with *Prorocentrum minimum*, yielding the best score in the BLASTn search. *Phaeocystis antarctica* was successfully identified during analysis, exhibiting high nucleotide identity (99.77% for 18S and 99.54% for 28S) with the homolog sequences of this species in the GenBank database. In conjunction, these results indicate that the dinoflagellate isolated in the present study belongs to the genus *Prorocentrum* and may represent a previously undescribed species. The formal description of this species is in process.

3.2. Experiment 1

The main objective of this experiment was to evaluate the response of *Phaeocystis antarctica* and *Prorocentrum* sp. to iron and vitamin B₁₂ limitation.

In the case of the *Prorocentrum* sp., the Chl-a content increased from 16.56 $\mu\text{g L}^{-1}$ (± 0.40) on Day 1 to 89.71 $\mu\text{g L}^{-1}$ (± 2.81) on Day 16 of the DFB treatment (Figure 3). The Fv/Fm ratio was recorded as 0.56 (± 0.02) on Day 1 and remained high until Day 8, before decreasing to 0.26 (± 0.02) on Day 16. An opposite trend was observed for σPSII at 440 nm, which increased from 8.48 nm^2 (± 0.18) on Day 1 to 10.10 nm^2 (± 0.20) on Day 8, and then decreased slightly to 8.82 nm^2 (± 0.19) on Day 16. In the -B12 treatment, the Chl-a content was maintained around 16.77 $\mu\text{g L}^{-1}$ (± 0.55) for the first seven days, before exhibiting a sharp increase to 132.22 $\mu\text{g L}^{-1}$ (± 2.78) on Day 16. The Fv/Fm ratio showed a similar trend to that of Chl-a, presenting a value of 0.57 (± 0.02) on Day 1 and remaining around ~ 0.54 until Day 8, before decreasing to 0.30 (± 0.02) at the end of the experiment (Figure 3). The σPSII at 440 nm increased from 8.22 nm^2 (± 0.18) on Day 1 to 10.20 nm^2 (± 0.20) on Day 11, and then decreased slightly to 9.33 (± 0.19) on Day 16. The Chl-a content and Fv/Fm in the CTRL treatment exhibited the same trend as in

the -B12 treatment. The Chl-a content exhibited the lowest value of $14.59 \mu\text{g L}^{-1}$ (± 0.52) on Day 1 and the highest value of $131.24 \mu\text{g L}^{-1}$ (± 2.67) on Day 16, whereas Fv/Fm ranged from 0.54 (± 0.02) on Day 1 to 0.29 (± 0.02) on Day 16. The σPSII at 440 nm ranged from 8.20 nm^2 (± 0.18) on Day 1 to 10.05 nm^2 (± 0.20) on Day 16 of this treatment (Figure 3).

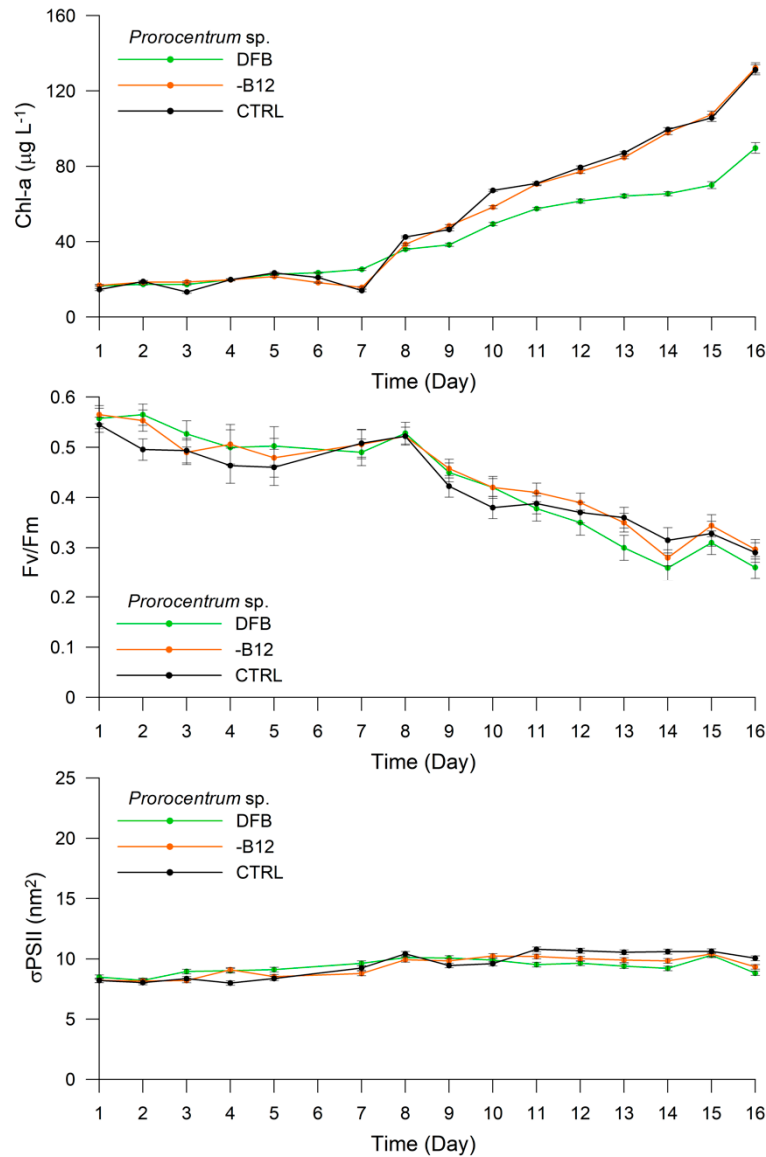


Figure 3. Experiment 1. Changes in chlorophyll-a (Chl-a) concentration ($\mu\text{g L}^{-1}$), maximum PSII photochemical efficiency (Fv/Fm), and maximum PSII effective absorption cross-section (σPSII) (nm^2) in *Prorocentrum* sp. under different treatments.

The total cell number increased from 15,000 to 58,000 cells mL^{-1} , 18,000 to 50,000 cells mL^{-1} , and 21,000 to 62,000 cells mL^{-1} in the DFB, -B12, and CTRL treatments, respectively, from the beginning to the end of the experiment. The pigment/Chl-a ratios for each treatment are presented in Table 1. The most significant differences were observed for the Chl- c_2 /Chl-a ratio among treatments, which were 0.36 (± 0.05), 0.34 (± 0.03), and 0.01 in the DFB, -B12, and CTRL treatments, respectively. The Perid/Chl-a ratio also differed among treatments, exhibiting values of 1.40 (± 0.02), 1.30 (± 0.05), and 1.27 (± 0.02) in the DFB, -B12, and CTRL treatment, respectively.

Table 1. Pigment:Chl-a ratios. **(A)** In *Prorocentrum* sp., *Phaeocystis antarctica*, and the mixed culture under different treatments in Experiment 1; **(B)** In *Prorocentrum* sp. and *Phaeocystis antarctica* under different light irradiances in Experiment 2. Abbreviations: Chl-a, chlorophyll-a; Chl-c₃, chlorophyll-c₃; Chl-c₂, chlorophyll-c₂; Perid, peridinin; But, 19'-butanoyloxyfucoxanthin; Fuco, fucoxanthin; Hex, 19'-hexanoyloxyfucoxanthin; Viola-like, violaxanthin-like pigment; Lut, lutein).

(A)														
	Lines Growth	Chl-c ₃ /Chl-a	Chl-c ₂ /Chl-a	Perid/Chl-a	But/Chl-a	Fuco/Chl-a	Hex/Chl-a	Viola-like/Chl-a	Lut/Chl-a	β-car/Chl-a	Hex: Chl-c ₂	Hex: Chl-c ₃	Perid: Hex	Dt/(Dd + Dt) × 100
<i>Prorocentrum</i> sp.	DFB	0.00	0.36	1.40	-	-	-	0.02	-	0.01	-	-	-	5.55
	-B12	0.00	0.34	1.30	-	-	-	0.03	-	0.01	-	-	-	4.75
	CTRL	0.03	0.01	1.27	-	-	-	0.03	-	0.01	-	-	-	4.62
<i>P. antarctica</i>	DFB	0.28	0.44	-	0.01	0.02	0.53	-	0.01	0.01	1.20	1.89	-	0
	-B12	0.24	0.35	-	0.01	0.02	0.47	-	0.01	0.01	1.33	1.94	-	0
	CTRL	0.26	0.38	-	0.01	0.02	0.42	-	0.01	0.01	1.11	1.63	-	0
Mixed culture	DFB	0.21	0.48	0.62	0.02	0.01	0.73	-	0.01	0.01	1.52	3.51	0.85	0.00
	-B12	0.20	0.43	0.93	0.00	0.00	0.21	-	0.00	0.01	0.49	1.04	4.43	2.78
	CTRL	0.08	0.37	0.88	0.00	0.00	0.21	-	0.00	0.01	0.56	2.45	4.19	0.00
(B)														
	Lines Growth	Chl-c ₃ /Chl-a	Chl-c ₂ /Chl-a	Perid/Chl-a	But/Chl-a	Fuco/Chl-a	Hex/Chl-a	Viola-like/Chl-a	Lut/Chl-a	β-car/Chl-a	Hex/Chl-c ₂	Hex/Chl-c ₃	Hex/Perid	Dt/(Dd + Dt) × 100
<i>Prorocentrum</i> sp.	HL	-	0.26	1.29	-	-	-	0.02	0.00	0.02	-	-	-	8.78
	L1	-	0.25	1.10	-	-	-	0.02	0.00	0.02	-	-	-	8.22
	L2	-	0.34	1.33	-	-	-	0.03	0.00	0.01	-	-	-	4.85
	L3	-	0.22	1.26	-	-	-	0.03	0.00	0.01	-	-	-	3.46
<i>P. antarctica</i>	HL	0.33	0.38	-	0.01	0.01	0.36	-	0.00	0.01	0.95	1.09	-	53.07
	L1	0.21	0.36	-	0.01	0.01	0.41	-	0.01	0.01	1.14	1.96	-	33.89
	L2	0.29	0.44	-	0.01	0.02	0.55	-	0.01	0.01	1.23	1.91	-	11.70
	L3	0.27	0.42	-	0.01	0.02	0.49	-	0.01	0.01	1.15	1.79	-	5.59

The response of *P. antarctica* in the DFB treatment presented a differential trend as compared with the -B12 and CTRL treatments (Figure 4). In the DFB treatment, the Chl-a content ranged from 8.98 $\mu\text{g L}^{-1}$ (± 0.34) on Day 1 to 196.98 $\mu\text{g L}^{-1}$ (± 2.98) on Day 16. On the contrary, Fv/Fm decreased from 0.41 (± 0.02) to 0.32 (± 0.02) in the first five days, and then remained constant until the end of the experiment. The σPSII at 440 nm increased from 15.98 nm^2 (± 0.27) on Day 1 to 17.14 nm^2 (± 0.29) on Day 16, peaking at 22.20 nm^2 (± 0.31) on Day 8. The Chl-a content in the -B12 treatment presented the same trend as that in the DFB treatment, varying from 8.35 $\mu\text{g L}^{-1}$ (± 0.34) on Day 1 to 160.68 $\mu\text{g L}^{-1}$ (± 3.30) on Day 16. The Fv/Fm ratio ranged between 0.39 (± 0.02) and 0.37 (± 0.02) during the first five days, exhibiting relatively low variability, and then stabilized at ~ 0.4 until the end of the experiment. The σPSII at 440 nm increased from 14.49 nm^2 (± 0.25) on Day 1 to 17.86 nm^2 (± 0.30) on Day 16, exhibiting fluctuations throughout the experiment. The Chl-a content in the CTRL treatment showed values ranging from 8.28 $\mu\text{g L}^{-1}$ (± 0.34) on Day 1 to 148.94 $\mu\text{g L}^{-1}$ (± 3.20) on Day 16. The Fv/Fm ratio also exhibited the same trend as in the -B12 treatment, albeit with lesser fluctuations and values ranging from 0.37 (± 0.02) on Day 1 to 0.40 (± 0.02) on Day 16. The σPSII at 440 nm was recorded as 16.38 (± 0.28) on Day 1 and 16.04 (± 0.28) on Day 16, peaking at 21.52 (± 0.26) on Day 7 and at 19.65 (± 0.21) on Day 9.

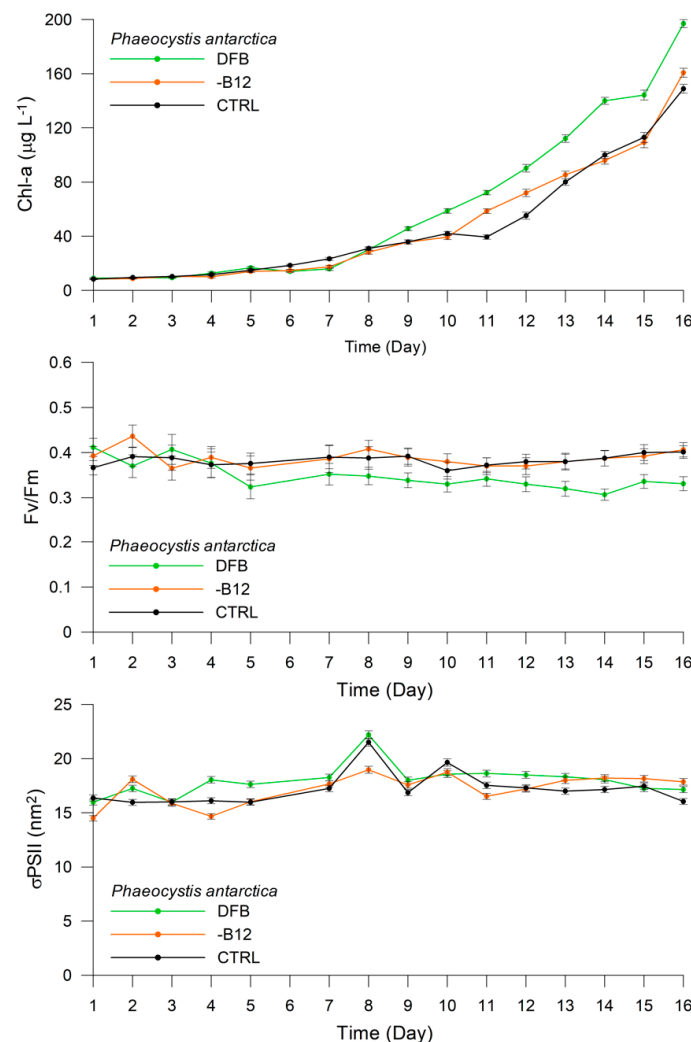


Figure 4. Experiment 1. Changes in Chl-a concentration ($\mu\text{g L}^{-1}$), Fv/Fm, and σPSII (nm^2) in *Phaeocystis antarctica* under different treatments.

The total cell number increased from 58,000 to 315,000 cells mL^{-1} , 45,000 to 230,000 cells mL^{-1} , and 48,000 to 252,500 cells mL^{-1} in the DFB, -B12, and CTRL treatments, respectively, from the beginning to the end of the experiment. The pigment/Chl-a ratios obtained by HPLC analyses are

presented in Table 1. The most significant differences were detected for Chl- c_2 /Chl- a and Hex/Chl- a ratios among treatments. The Chl- c_2 /Chl- a ratio was 0.44 (± 0.01), 0.35 (± 0.01), and 0.38 (± 0.01), whereas the Hex/Chl- a ratio was 0.53 (± 0.02), 0.47 (± 0.02), and 0.42 (± 0.01) in the DFB, -B12, and CTRL treatments, respectively.

The trends exhibited by the measured variables in the mixed culture were more similar to *Prorocentrum* sp. (Figure 5) The Chl- a content ranged from 5.50 $\mu\text{g L}^{-1}$ (± 0.13) on Day 1 to 58.28 $\mu\text{g L}^{-1}$ (± 1.07) on Day 16 of the DFB experiment, with a lag phase in the first week during which the values ranged from 5.50 $\mu\text{g L}^{-1}$ to 8.89 $\mu\text{g L}^{-1}$ (± 0.34). The Fv/Fm ratio varied between 0.44 (± 0.02) and 0.41 (± 0.01) during the first eight days, before decreasing to 0.23 (± 0.02) on Day 16. The σPSII at 440 nm ranged between 11.06 (± 0.20) on Day 1 and 11.32 (± 0.25) on Day 16, with relatively fluctuating values and a peak of 15.40 (± 0.23) on Day 10. The increase in Chl- a was lower in the -B12 treatment than in the DFB treatment, with values ranging from 6.25 $\mu\text{g L}^{-1}$ (± 0.08) on Day 1 to 43.86 $\mu\text{g L}^{-1}$ (± 0.98) on Day 16. The Fv/Fm ratio ranged from 0.43 (± 0.01) on Day 1 to 0.34 (± 0.02) on Day 16, exhibiting relatively high variability during the first week. In contrast to the DFB treatment, σPSII at 440 nm increased from 10.81 (± 0.22) on Day 1 to 14.04 (± 0.25) on Day 16, exhibiting considerable fluctuations. The Chl- a content ranged from 5.29 $\mu\text{g L}^{-1}$ (± 0.06) on Day 1 to 40.27 $\mu\text{g L}^{-1}$ (± 0.97) on Day 16 in the CTRL treatment, whereas Fv/Fm varied between 0.41 (± 0.02) on Day 1 and 0.37 (± 0.02) on Day 16, presenting a similar trend to that observed in the DFB treatment, and σPSII at 440 nm increased from 12.16 (± 0.22) on Day 1 to 15.98 (± 0.27) on Day 16, peaking at 17.25 (± 0.43) on Day 8 (Figure 5).

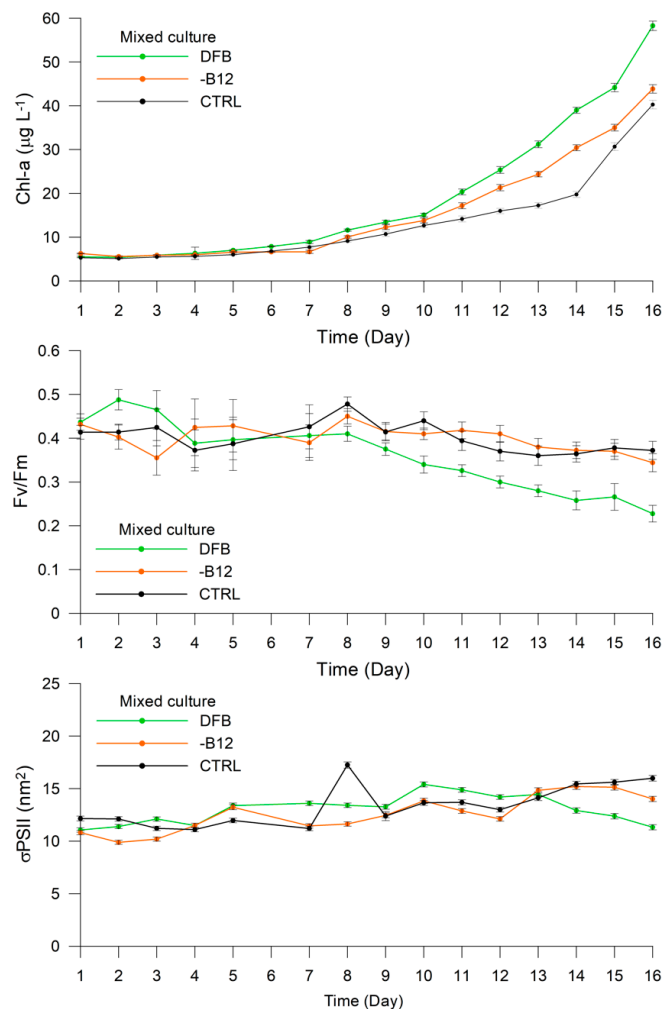


Figure 5. Experiment 1. Changes in Chl- a concentration ($\mu\text{g L}^{-1}$), Fv/Fm, and σPSII (nm^2) in the mixed culture of *Phaeocystis antarctica* and *Prorocentrum* sp. under different treatments.

The Perid/Hex ratio was used as a proxy in the HPLC analysis to determine the dominant phytoplankton, i.e., *P. antarctica* or *Prorocentrum* sp., in the three treatments (Table 1). This ratio was recorded as 4.25 (± 0.01), 4.44 (± 0.02), and (± 0.02) in the CTRL, -B12, and DFB treatments.

3.3. Experiment 2

The *Prorocentrum* sp. and *Phaeocystis antarctica* responded differently to different light intensities (HL, L1, L2, and L3) (Figures 6 and 7). The Chl-a content of *Prorocentrum* sp. increased from 15.25 $\mu\text{g L}^{-1}$ (± 0.42) on Day 1 to 81.60 $\mu\text{g L}^{-1}$ (± 2.15) on Day 16 in the HL treatment (Figure 6). The Fv/Fm ratio decreased remarkably from 0.45 (± 0.02) on Day 1 to 0.01 (± 0.01) on Day 16, whereas σPSII remained almost constant throughout the experiment, varying from 8.24 to 8.05 (± 0.24), except on Day 16 when it exhibited the lowest value of 5.98 (± 0.21). The Chl-a content and Fv/Fm in the L1 treatment exhibited a similar trend to that in the HL treatment. The Chl-a content increased from 17.43 $\mu\text{g L}^{-1}$ (± 0.36) on Day 1 to 113.53 $\mu\text{g L}^{-1}$ (± 2.12) on Day 16, whereas Fv/Fm decreased from 0.51 (± 0.03) on Day 1 to 0.09 (± 0.02) on Day 16. The σPSII values remained almost constant with very few fluctuations, varying between 8.51 (± 0.18) and 7.81 (± 0.18). In the L2 treatment, the Chl-a content ranged from 16.41 $\mu\text{g L}^{-1}$ (± 0.31) on Day 1 to 157.29 $\mu\text{g L}^{-1}$ (± 1.39) on Day 16, whereas Fv/Fm decreased from 0.52 (± 0.03) on Day 1 to 0.20 (± 0.02) on Day 16, presenting values higher than those obtained in the HL and L1 treatments. The σPSII values increased slightly from 8.71 (± 0.18) on Day 1 to 9.57 (± 0.19) on Day 16, peaking at 11.42 (± 0.20) on Day 11. In the L3 treatment with the lowest irradiance, the Chl-a content increased from 17.28 $\mu\text{g L}^{-1}$ (± 0.13) on Day 1 to 171.24 $\mu\text{g L}^{-1}$ (± 1.03) on Day 16. The Fv/Fm ratio decreased slightly from 0.52 (± 0.02) on Day 1 to 0.26 (± 0.02) on Day 16, whereas σPSII remained constant during the first eight days (8.17–8.35), increasing up to 10.42–10.77 (± 0.20) between Days 9 and 15, and reaching 9.67 (± 0.19) at the end of the experiment. The total cell number increased from 41,000 to 517,500 cells mL^{-1} , 35,384 to 452,500 cells mL^{-1} , 31,111 to 465,000 cells mL^{-1} , and 55,000 to 267,500 cells mL^{-1} in the HL, L1, L2, and L3 treatments, respectively, from the beginning to the end of the experiment (Figure 6).

Phaeocystis antarctica exhibited less variability than *Prorocentrum* sp. under all light intensities (Figure 7). In the HL treatment, the Chl-a content increased from 7.48 $\mu\text{g L}^{-1}$ (± 0.23) on Day 1 to 104.69 $\mu\text{g L}^{-1}$ (± 1.35) on Day 16, whereas Fv/Fm ranged from 0.24 (± 0.02) on Day 1 to 0.38 (± 0.01) on Day 16. The σPSII remained almost constant during the 16 days, ranging between 13.39 (± 0.24) and 11.28 (± 0.21). In the L1 treatment, the Chl-a content increased from 8.27 $\mu\text{g L}^{-1}$ (± 0.23) on day 1 to 120.15 $\mu\text{g L}^{-1}$ (± 1.24) on Day 16, with Fv/Fm ranging between 0.23 (± 0.01) and 0.38 (± 0.02), consistent with that observed in the HL treatment, albeit with less variability. The σPSII remained constant at ~ 15.9 for the first 10 days, before increasing to 18.41 (± 0.23) on Day 13, and then reaching 13.24 (± 0.21) at the end of the experiment. In the L2 treatment, the Chl-a content increased from 8.46 $\mu\text{g L}^{-1}$ (± 0.13) on Day 1 to 136.41 $\mu\text{g L}^{-1}$ (± 1.35) on Day 16, while Fv/Fm increased from 0.29 (± 0.01) to 0.36 (± 0.02). The σPSII increased from 14.43 (± 0.25) to 18.26 (± 0.31) during the first 11 days, and then decreased slightly to 15.65 (± 0.27) on Day 16. In the L3 treatment, the Chl-a content remained low in the first seven days, ranging from 8.46 $\mu\text{g L}^{-1}$ (± 0.13) to 13.70 $\mu\text{g L}^{-1}$ (± 1.30), and then increased remarkably to 169.01 $\mu\text{g L}^{-1}$ (± 0.30) on Day 16. The Fv/Fm ratio remained almost constant throughout the experiment, with values ranging between 0.39 (± 0.02) and 0.37 (± 0.02). Similarly, the σPSII also remained almost constant, varying between 16.12 (± 0.28) and 16.23 (± 0.28) (Figure 7).

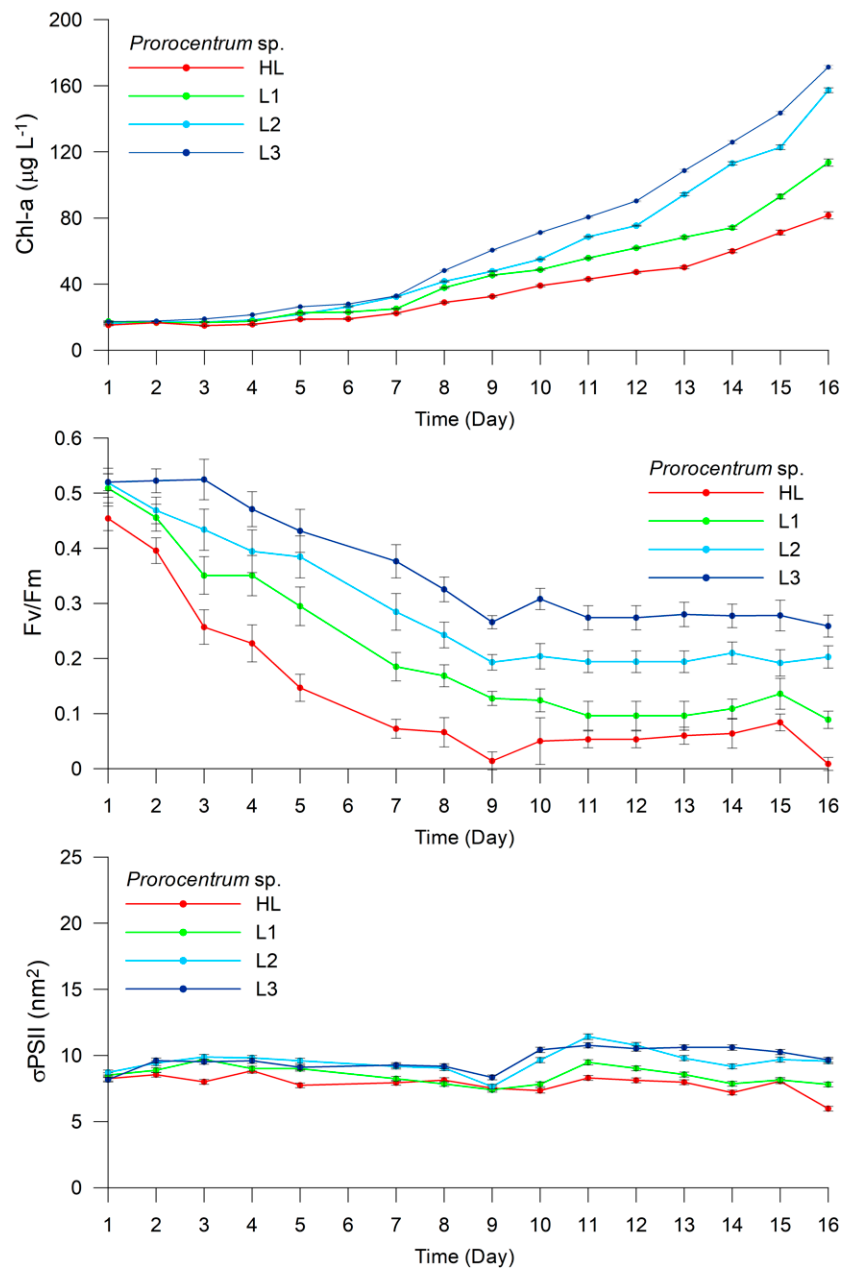


Figure 6. Experiment 2. Changes in Chl-a concentration ($\mu\text{g L}^{-1}$), Fv/Fm, and σPSII (nm^2) in *Prorocentrum* sp. under different light intensities (high light (HL), low light 1 (L1), low light 2 (L2), and low light 3 (L3)).

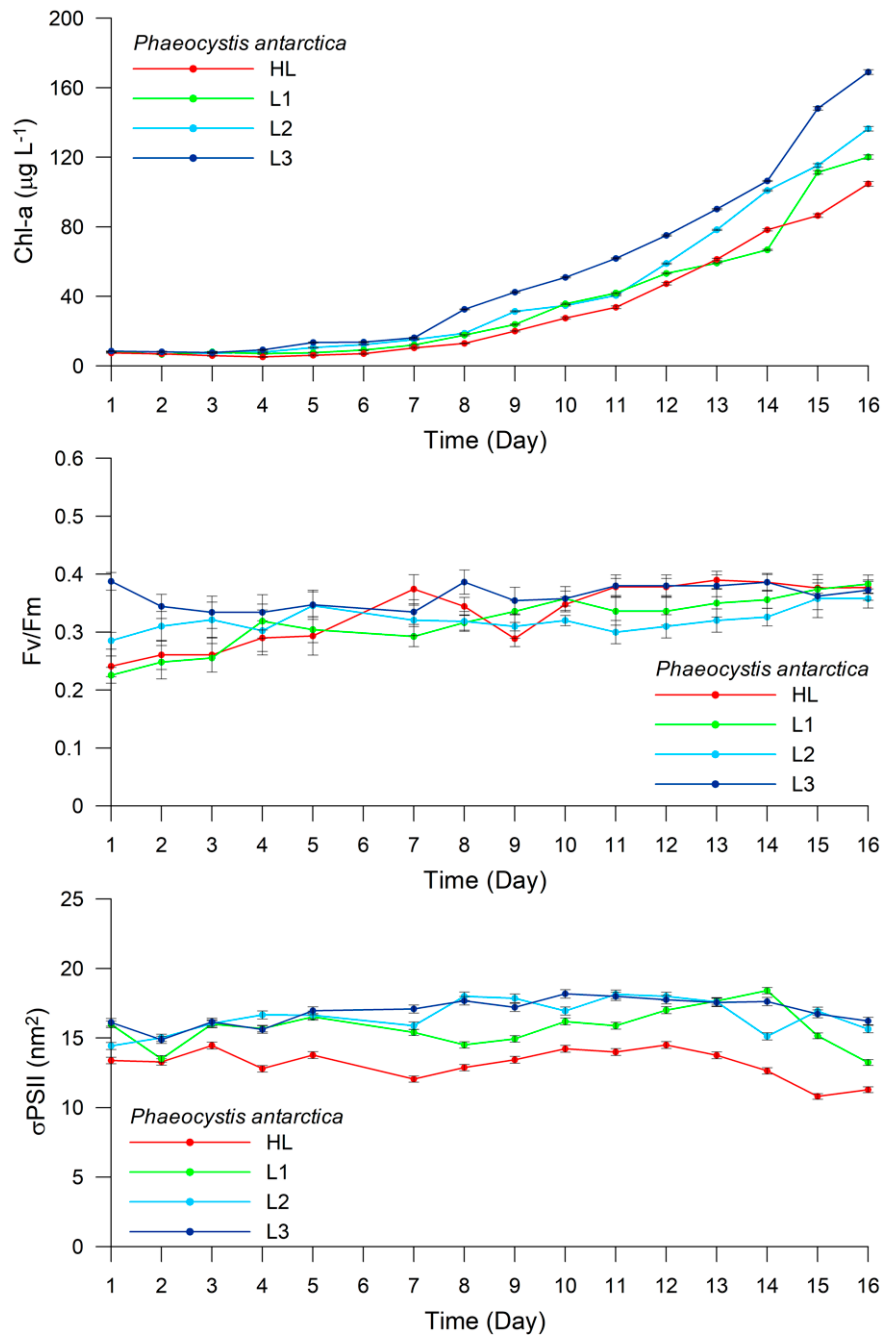


Figure 7. Experiment 2. Changes in Chl-a concentration ($\mu\text{g L}^{-1}$), Fv/Fm, and σPSII (nm^2) in *Phaeocystis antarctica* under different light intensities (HL, L1, L2, and L3).

Results of the HPLC analyses revealed high variability among the treatments in terms of their $Dt/(Dd + Dt) \times 100$ value. For *Prorocentrum* sp., this value was 8.8%, 8.2%, 4.9%, and 3.5% in the HL, L1, L2, and L3 treatments, respectively. However, these values were remarkably high for *P. antarctica*, calculated as 53.1%, 33.9%, 11.7%, and 5.6% in the HL, L1, L2, and L3 treatments, respectively, and exhibited considerable differences, as evident in Table 1.

The total cell number increased from 20,000 to 50,000 cells mL^{-1} , 17,000 to 68,000 cells mL^{-1} , 15,000 to 98,000 cells mL^{-1} , and 20,000 to 62,000 cells mL^{-1} in the HL, L1, L2, and L3 treatments, respectively, from the beginning to the end of the experiment.

4. Discussion

Considering the role of dissolved iron in modulating the primary productivity of the Antarctic waters, the main objective of this work was to describe the responses and relationships between a new species of *Prorocentrum* sp. and *Phaeocystis antarctica* under iron and vitamin B₁₂ limitation, and the consequent ecological implications for Antarctic waters. The redistribution of dissolved iron in the Ross Sea is one of the most debated concepts in Antarctic ecology, and the ability of the phytoplankton community to respond rapidly to environmental changes renders it crucial in the monitoring of marine environment and the transfer of carbon to higher trophic levels. The spatial and temporal differences among diatoms and haptophyte blooms in the Ross Sea have been correlated to the differential ability of species to grow under varying environmental conditions, such as light availability or iron and vitamin B₁₂ co-limitation, which could potentially shape the phytoplankton community structure [9,17,60–62]. The dominance of *P. antarctica* in early spring, in the presence of a deep mixed layer and nonlimiting iron concentrations, has been attributed to its ability to photosynthesize efficiently under low irradiance by increasing the Chl-a content and iron uptake. Furthermore, [18] demonstrated that the iron threshold of *P. antarctica* was 100 times lower than that of the diatoms (e.g., *Chaetoceros* sp.), and that high light and iron availability could trigger colony formation. In spite of the numerous studies on the processes involved in colony formation, the trophic fate of mucilaginous colonies remains poorly known [14,18,63–65]. In view of the significant ecological implications of these, the isolation and identification of a new *Prorocentrum* sp. from colonies of *P. antarctica* prompted us to investigate the relationship between the two species under iron and vitamin B₁₂ limitation. We further compared the responses of the two species with different levels of irradiance without nutrient limitation. Laboratory studies conducted under controlled conditions have demonstrated the effect of light, iron, and iron and vitamin B₁₂ co-limitation on *P. antarctica*, including mechanisms involved in colony formation, in cells preadapted to different growing conditions for weeks [9,18,61]. In this study, isolates were initially grown under nutrient availability, and then exposed to limitation conditions at the maximum growth rate. Overall, the results illustrated the differential photosynthesizing ability of the two species under high levels of irradiance (Figure 8).

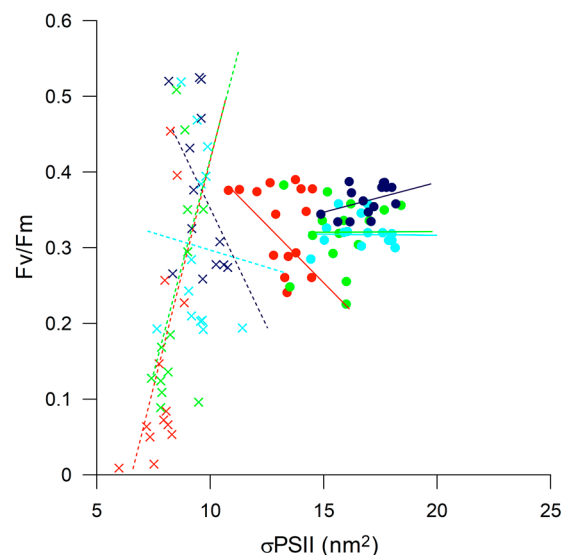


Figure 8. Fv/Fm plotted against relative functional absorption cross-section of PSII (σ_{PSII}) for *Prorocentrum* sp. (symbol X) and *Phaeocystis antarctica* (symbol ●) with color indicating different levels of irradiance. Red (HL), light green (L1), light blue (L2), and blue (L3). The figure includes all data points with trend lines.

Prorocentrum sp. was unable to photosynthesize efficiently under light exceeding 60 mmol photons $\text{m}^{-2} \text{s}^{-1}$, as indicated by Fv/Fm ~ 0.01 and slight changes in σ_{PSII} , with the $\text{Dt}/(\text{Dd} + \text{Dt}) \times 100$ value

2.5 times higher in HL than in the L3 treatment. In contrast, *P. antarctica* was able to regulate the functional optical cross-section of σ PSII in relation to different irradiance levels, maintaining high Fv/Fm under varying light intensity, with the $Dt/(Dd + Dt) \times 100$ value 9.5 times higher in HL than in the L3 treatment. We noted that a Viola-like pigment increased at high light intensity in *Prorocentrum* sp., and it is known that violaxanthin is involved in the xanthophyll cycle under prolonged high light stress [66].

P. antarctica and *Prorocentrum* sp. responded differently to iron and vitamin B₁₂ limitation. *Prorocentrum* sp. exhibited a lower increase in the Chl-a content in the DFB than in the -B12 and CTRL treatments, as well as a lower Chl-a/cell ratio (Table 1). In contrast, differences among treatments were less evident for Fv/Fm and σ PSII, with the former exhibiting a slight decrease during the experiment, whereas the latter remained almost constant (Figure 9).

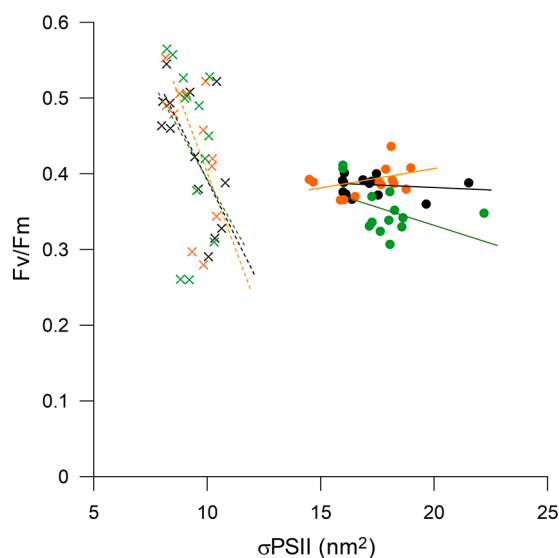


Figure 9. Fv/Fm plotted against relative functional absorption cross-section of PSII (σ PSII) for *Prorocentrum* sp. (symbol X) and *Phaeocystis antarctica* (symbol ●) with color indicating different treatments. CTRL (black), -B12 (orange), DFB (green). The figure includes all data points with trend lines.

P. antarctica presented an opposite trend, with a greater increase in both the Chl-a content and Fv/Fm in the DFB treatment. However, Fv/Fm did not exhibit considerable variation, and σ PSII was observed to be similar among the treatments, remaining almost constant throughout the experiment. The highest Chl-a/cell ratio was observed in the -B12 treatment, with smaller differences among the treatments than those detected for *Prorocentrum* sp. These results suggest that both these species are more sensitive to changes in the dissolved iron availability than to B₁₂. The increase in Chl-a observed in *P. antarctica* could reflect the dissolution of colonies (data not shown) under iron limitation, thus “conserving” the energy required for colony formation and resulting in an increase in the single cell morphotype. The lower iron threshold and ability of *P. antarctica* colonies to chelate iron has been well documented, and similar trends of photosynthetic parameters observed in the DFB treatment have suggested that this species was not affected by iron limitation, likely due to mucus storage. It has been estimated that approximately 50%–80% of the *Phaeocystis* carbon content was present in the extracellular mucilaginous matrix [21,22,67,68], which improved the ability of the colony to sequester micronutrients (e.g., iron) [14,69] and function as a microbiome and vitamin B₁₂ source [9]. The Perid/Hex ratio, used as a proxy to determine the dominant phytoplankton in mixed cultures, was lower in the DFB treatment, indicating the ability of colonial *Phaeocystis* to grow well even under iron limitation. A change was noted in the color of dissociating colonies in the DFB treatment (data not shown). This phenomenon warrants further investigation, considering the poor digestibility of the

mucus and low grazing pressure on colonies, which allow for efficient export of carbon to the bottom of the ocean.

The presence of dinoflagellates in the marine environment has been correlated to water column stability or nutrient deficiency [70,71]. Of the mixotrophic species, food vacuoles or prey ingestion have been observed in Prorocentrales, particularly in *Prorocentrum minimum* [72], and the host species of dinoflagellates within the mucilaginous colonies of *P. antarctica* have been previously reported [30,73]. In addition, a novel dinoflagellate, related to the ichthyotoxic genera *Karenia* and *Karlodinium*, discovered in the Ross Sea by [74] was closely related to the free-living, unicellular *P. antarctica*. Although it is not clear if kleptoplastic dinoflagellates prefer colonial or unicellular stages of *P. antarctica* as the plastid source [30,31], the important ecological role of mixotrophy in providing access to limiting nutrients has long been recognized [75–77], as it has significantly impacted prey populations in marine microbial food webs.

The Ross Sea is considered to be the most productive region in the Southern Ocean, playing a key role in the transfer of atmospheric carbon to the ocean's interior and in global climate regulation. The phytoplankton bloom dynamics in the region have been well documented, with communities dominated mainly by diatoms and the *P. antarctica*, which can form almost monospecific blooms with distinctive biogeochemical imprints due to their differential metabolism and trophic fate. However, the drivers regulating these blooms remain unclear, particularly in view of recent changes in the physical and biological properties of the Ross Sea. The discovery of novel dinoflagellate species [31,78], high abundance of loricate choanoflagellates [26], and changes in the level of productivity in the Ross Sea highlight the importance of spatial assessments of phytoplankton community structure and dynamics [79], which may lead to the discovery of additional, enabling better modeling of the phytoplankton community, with important ecological implications for the Antarctic food web and biogeochemical cycles in the Southern Ocean [80].

5. Conclusions

The isolation and identification of a new *Prorocentrum* sp. from colonial *Phaeocystis antarctica* are important for ecological studies of the Ross Sea. The inability of this new species to photosynthesize efficiently under high irradiance and reduced growth under iron limitation provides a basis for future investigations on its relationship with *P. antarctica*. In view of the current shifts in climate regimes, the discovery of this new species supports the re-evaluation of the role of dinoflagellates in the Antarctic food web and biogeochemical processes in one of the most important regions for the global energy budget. Considering the tendency of dinoflagellates to feed on external organic sources, our results provide new perspectives on the study of the phytoplankton communities of the Ross Sea, particularly under changing climatic conditions.

Author Contributions: Conceptualization, F.B. and O.M.; methodology, F.B., M.S., A.C., E.S. and M.C.V.; validation, S.A. and O.M.; formal analysis, F.B., S.A. and M.C.V.; investigation, O.M.; data curation, F.B. and O.M.; writing—original draft preparation, F.B., S.A. and O.M.; writing—review and editing, F.B., M.S., S.A., A.C., M.C.V. and O.M.; funding acquisition, O.M. All authors have read and agreed to the published version of the manuscript.

Funding: This study was funded by the Italian National Program for Antarctic Research, under the Projects P-ROSE (PNRA16_00239) and CELEBeR (PNRA16_00207).

Acknowledgments: The authors express their gratitude to the Italian Antarctic National Program (PNRA) and the scientific personnel and crew of the R/V *Italica* for their logistical support. The authors are also grateful to CoNISMa for continuous administrative support. The authors thank Antonino De Natale for support during field sampling, and Mario Affuso for technical support in the laboratory. Thanks to Carmelo R. Tomas and Gian Carlo Carrada for their valuable and constructive criticism and suggestions during manuscript preparation.

Conflicts of Interest: The authors declare no conflict of interest.

References

1. Smith, W.O.; Nelson, D.M. Phytoplankton Bloom Produced by a Receding Ice Edge in the Ross Sea: Spatial Coherence with the Density Field. *Science* **1985**, *227*, 163–166. [[CrossRef](#)] [[PubMed](#)]
2. Arrigo, K.R. Phytoplankton Community Structure and the Drawdown of Nutrients and CO₂ in the Southern Ocean. *Science* **1999**, *283*, 365–367. [[CrossRef](#)] [[PubMed](#)]
3. Peloquin, J.A.; Smith, W.O. Phytoplankton blooms in the Ross Sea, Antarctica: Interannual variability in magnitude, temporal patterns, and composition. *J. Geophys. Res.* **2007**, *112*, C08013. [[CrossRef](#)]
4. Tremblay, J.-E.; Smith, W.O. Chapter 8 Primary Production and Nutrient Dynamics in Polynyas. In *Polynyas: Windows to the World*; Smith, W.O., Barber, D.G., Eds.; Elsevier Oceanography Series; Elsevier: Amsterdam, The Netherlands, 2007; Volume 74, pp. 239–269. [[CrossRef](#)]
5. Smith, W.O.; Ainley, D.G.; Arrigo, K.R.; Dinniman, M.S. The Oceanography and Ecology of the Ross Sea. *Annu. Rev. Mar. Sci.* **2014**, *6*, 469–487. [[CrossRef](#)] [[PubMed](#)]
6. Smith, W.O.; Shields, A.R.; Peloquin, J.A.; Catalano, G.; Tozzi, S.; Dinniman, M.S.; Asper, V.A. Interannual variations in nutrients, net community production, and biogeochemical cycles in the Ross Sea. *Deep Sea Res. Part II Top. Stud. Oceanogr.* **2006**, *53*, 815–833. [[CrossRef](#)]
7. DiTullio, G.R.; Smith, W.O. Spatial patterns in phytoplankton biomass and pigment distributions in the Ross Sea. *J. Geophys. Res. Oceans* **1996**, *101*, 18467–18477. [[CrossRef](#)]
8. Smith, W.O.; Marra, J.; Hiscock, M.R.; Barber, R.T. The seasonal cycle of phytoplankton biomass and primary productivity in the Ross Sea, Antarctica. *Deep Sea Res. Part II Top. Stud. Oceanogr.* **2000**, *47*, 3119–3140. [[CrossRef](#)]
9. Bertrand, E.M.; Saito, M.A.; Rose, J.M.; Riesselman, C.R.; Lohan, M.C.; Noble, A.E.; Lee, P.A.; DiTullio, G.R. Vitamin B₁₂ and iron colimitation of phytoplankton growth in the Ross Sea. *Limnol. Oceanogr.* **2007**, *52*, 1079–1093. [[CrossRef](#)]
10. Bertrand, E.M.; McCrow, J.P.; Moustafa, A.; Zheng, H.; McQuaid, J.B.; Delmont, T.O.; Post, A.F.; Sipler, R.E.; Spackeen, J.L.; Xu, K.; et al. Phytoplankton–bacterial interactions mediate micronutrient colimitation at the coastal Antarctic sea ice edge. *Proc. Natl. Acad. Sci. USA* **2015**, *112*, 9938–9943. [[CrossRef](#)] [[PubMed](#)]
11. Tang, Y.Z.; Koch, F.; Gobler, C.J. Most harmful algal bloom species are vitamin B₁ and B₁₂ auxotrophs. *Proc. Natl. Acad. Sci. USA* **2010**, *107*, 20756–20761. [[CrossRef](#)] [[PubMed](#)]
12. Koch, F.; Marcoval, M.A.; Panzeca, C.; Bruland, K.W.; Sañudo-Wilhelmy, S.A.; Gobler, C.J. The effect of vitamin B₁₂ on phytoplankton growth and community structure in the Gulf of Alaska. *Limnol. Oceanogr.* **2011**, *56*, 1023–1034. [[CrossRef](#)]
13. Delmont, T.O.; Hammar, K.M.; Ducklow, H.W.; Yager, P.L.; Post, A.F. *Phaeocystis antarctica* blooms strongly influence bacterial community structures in the Amundsen Sea polynya. *Front. Microbiol.* **2014**, *5*. [[CrossRef](#)] [[PubMed](#)]
14. Schoemann, V.; Becquevort, S.; Stefels, J.; Rousseau, V.; Lancelot, C. *Phaeocystis* blooms in the global ocean and their controlling mechanisms: A review. *J. Sea Res.* **2005**, *53*, 43–66. [[CrossRef](#)]
15. Sedwick, P.N.; Garcia, N.S.; Riseman, S.F.; Marsay, C.M.; DiTullio, G.R. Evidence for high iron requirements of colonial *Phaeocystis antarctica* at low irradiance. *Biogeochemistry* **2007**, *83*, 83–97. [[CrossRef](#)]
16. Garcia, N.; Sedwick, P.; DiTullio, G. Influence of irradiance and iron on the growth of colonial *Phaeocystis antarctica*: Implications for seasonal bloom dynamics in the Ross Sea, Antarctica. *Aquat. Microb. Ecol.* **2009**, *57*, 203–220. [[CrossRef](#)]
17. Alderkamp, A.-C.; Kulk, G.; Buma, A.G.J.; Visser, R.J.W.; Van Dijken, G.L.; Mills, M.M.; Arrigo, K.R. The effect of iron limitation on the photophysiology of *Phaeocystis antarctica* (Prymnesiophyceae) and *Fragilariopsis cylindrus* (Bacillariophyceae) under dynamic irradiance. *J. Phycol.* **2012**, *48*, 45–59. [[CrossRef](#)]
18. Bender, S.J.; Moran, D.M.; McIlvin, M.R.; Zheng, H.; McCrow, J.P.; Badger, J.; DiTullio, G.R.; Allen, A.E.; Saito, M.A. Colony formation in *Phaeocystis antarctica*: Connecting molecular mechanisms with iron biogeochemistry. *Biogeosciences* **2018**, *15*, 4923–4942. [[CrossRef](#)]
19. Mathiot, P.; Jourdain, N.C.; Barnier, B.; Gallée, H.; Molines, J.M.; Le Sommer, J.; Penduff, T. Sensitivity of coastal polynyas and high-salinity shelf water production in the Ross Sea, Antarctica, to the atmospheric forcing. *Ocean Dyn.* **2012**, *62*, 701–723. [[CrossRef](#)]

20. Dennett, M.R.; Mathot, S.; Caron, D.A.; Smith, W.O.; Lonsdale, D.J. Abundance and distribution of phototrophic and heterotrophic nano- and microplankton in the southern Ross Sea. *Deep Sea Res. Part II Top. Stud. Oceanogr.* **2001**, *48*, 4019–4037. [[CrossRef](#)]
21. Rousseau, V.; Chrétiennot-Dinet, M.-J.; Jacobsen, A.; Verity, P.; Whipple, S. The life cycle of *Phaeocystis*: State of knowledge and presumptive role in ecology. *Biogeochemistry* **2007**, *83*, 29–47. [[CrossRef](#)]
22. Hamm, C.; Simson, D.; Merkel, R.; Smetacek, V. Colonies of *Phaeocystis globosa* are protected by a thin but tough skin. *Mar. Ecol. Prog. Ser.* **1999**, *187*, 101–111. [[CrossRef](#)]
23. Andreoli, C.; Tolomio, C.; Moro, I.; Radice, M.; Moschin, E.; Bellato, S. Diatoms and dinoflagellates in Terra Nova Bay (Ross Sea-Antarctica) during austral summer 1990. *Polar Biol.* **1995**, *15*. [[CrossRef](#)]
24. Waters, R.L.; van den Enden, R.; Marchant, H.J. Summer microbial ecology off East Antarctica (80–150° E): Protistan community structure and bacterial abundance. *Deep Sea Res. Part II Top. Stud. Oceanogr.* **2000**, *47*, 2401–2435. [[CrossRef](#)]
25. Davidson, A.T.; Scott, F.J.; Nash, G.V.; Wright, S.W.; Raymond, B. Physical and biological control of protistan community composition, distribution and abundance in the seasonal ice zone of the Southern Ocean between 30 and 80° E. *Deep Sea Res. Part II Top. Stud. Oceanogr.* **2010**, *57*, 828–848. [[CrossRef](#)]
26. Escalera, L.; Mangoni, O.; Bolinesi, F.; Saggiomo, M. Austral Summer Bloom of Loricated Choanoflagellates in the Central Ross Sea Polynya. *J. Eukaryot. Microbiol.* **2019**, *66*, 849–852. [[CrossRef](#)] [[PubMed](#)]
27. Balech, E. Contribución al conocimiento del plancton antártico. Plancton del Mar de Bellingshausen. *Physis* **1947**, 75–91.
28. Balech, E. Clave ilustrada de dinoflagelados antárticos. *Publ. Inst. Antárt. Argent.* **1976**, *11*, 1–99.
29. Gast, R.J.; Moran, D.M.; Dennett, M.R.; Caron, D.A. Kleptoplasty in an Antarctic dinoflagellate: Caught in evolutionary transition? *Environ. Microbiol.* **2007**, *9*, 39–45. [[CrossRef](#)]
30. Stamatakis, K.; Broussos, P.-I.; Panagiotopoulou, A.; Gast, R.J.; Pelecanou, M.; Papageorgiou, G.C. Light-adaptive state transitions in the Ross Sea haptophyte *Phaeocystis antarctica* and in dinoflagellate cells hosting kleptoplasts derived from it. *Biochim. Biophys. Acta BBA—Bioenerg.* **2019**, *1860*, 102–110. [[CrossRef](#)]
31. Phan-Tan, L.; Nguyen-Ngoc, L.; Smith, W.O.; Doan-Nhu, H. A new dinoflagellate species, *Protoperidinium smithii* H. Doan-Nhu, L. Phan-Tan et L. Nguyen-Ngoc sp. nov., and an emended description of *Protoperidinium defectum* (Balech 1965) Balech 1974 from the Ross Sea, Antarctica. *Polar Biol.* **2018**, *41*, 983–992. [[CrossRef](#)]
32. DiTullio, G.R.; Smith, W.O. Relationship between dimethylsulfide and phytoplankton pigment concentrations in the Ross Sea, Antarctica. *Deep Sea Res. Part Oceanogr. Res. Pap.* **1995**, *42*, 873–892. [[CrossRef](#)]
33. DiTullio, G.R.; Grebmeier, J.M.; Arrigo, K.R.; Lizotte, M.P.; Robinson, D.H.; Leventer, A.; Barry, J.P.; VanWoert, M.L.; Dunbar, R.B. Rapid and early export of *Phaeocystis antarctica* blooms in the Ross Sea, Antarctica. *Nature* **2000**, *404*, 595–598. [[CrossRef](#)] [[PubMed](#)]
34. Wright, S.; Thomas, D.; Marchant, H.; Higgins, H.; Mackey, M.; Mackey, D. Analysis of phytoplankton of the Australian sector of the Southern Ocean: Comparisons of microscopy and size frequency data with interpretations of pigment HPLC data using the “CHEMTAX” matrix factorisation program. *Mar. Ecol. Prog. Ser.* **1996**, *144*, 285–298. [[CrossRef](#)]
35. Roy, S.; Llewellyn, C.; Egeland, E.S.; Johnsen, G. (Eds.) *Phytoplankton Pigments: Characterization, Chemotaxonomy and Applications in Oceanography*; Cambridge University Press: Cambridge, UK, 2011; p. 845. ISBN 978-0-511-73226-3.
36. Mangoni, O.; Saggiomo, V.; Bolinesi, F.; Margiotta, F.; Budillon, G.; Cotroneo, Y.; Misic, C.; Rivaro, P.; Saggiomo, M. Phytoplankton blooms during austral summer in the Ross Sea, Antarctica: Driving factors and trophic implications. *PLoS ONE* **2017**, *12*, e0176033. [[CrossRef](#)]
37. Doyle, J.J.; Doyle, J. Isolation of plant DNA from fresh tissue. *Focus* **1999**, 13–15.
38. Wakeman, K.C.; Yamaguchi, A.; Horiguchi, T. Molecular Phylogeny and Morphology of *Haplozoon ezoense* n. sp. (Dinophyceae): A Parasitic Dinoflagellate with Ultrastructural Evidence of Remnant Non-photosynthetic Plastids. *Protist* **2018**, *169*, 333–350. [[CrossRef](#)] [[PubMed](#)]
39. Scholin, C.A.; Herzog, M.; Sogin, M.; Anderson, D.M. Identification of group- and strain-specific genetic markers for globally distributed *Alexandrium* (Dinophyceae). II. Sequence analysis of a fragment of the LSU Rrna Gene1. *J. Phycol.* **1994**, *30*, 999–1011. [[CrossRef](#)]

40. Vandersea, M.W.; Kibler, S.R.; Holland, W.C.; Tester, P.A.; Schultz, T.F.; Faust, M.A.; Holmes, M.J.; Chinain, M.; Wayne Litaker, R. Development of semi-quantitative pcr assays for the detection and enumeration of *Gambierdiscus* species (Gonyaulacales, dinophyceae)1: *Gambierdiscus* qPCR. *J. Phycol.* **2012**, *48*, 902–915. [[CrossRef](#)]
41. Nakayama, T.; Watanabe, S.; Mitsui, K.; Uchida, H.; Inouye, I. The phylogenetic relationship between the Chlamydomonadales and Chlorococcales inferred from 18SrDNA sequence data. *Phycol. Res.* **1996**, *44*, 47–55. [[CrossRef](#)]
42. Aceto, S.; Caputo, P.; Cozzolino, S.; Gaudio, L.; Moretti, A. Phylogeny and Evolution of Orchis and Allied Genera Based on ITS DNA Variation: Morphological Gaps and Molecular Continuity. *Mol. Phylogenet. Evol.* **1999**, *13*, 67–76. [[CrossRef](#)]
43. Kogame, K.; Horiguchi, T.; Masuda, M. Phylogeny of the order Scytosiphonales (Phaeophyceae) based on DNA sequences of *rbcL*, partial *rbcS*, and partial LSU nrDNA. *Phycologia* **1999**, *38*, 496–502. [[CrossRef](#)]
44. Hallegraeff, G.M.; Anderson, D.M.; Cembella, A.D. *Manual on Harmful Marine Microalgae*; UNESCO Publishing: Paris, France, 2004; ISBN 978-92-3-103948-5.
45. Holm-Hansen, O.; Lorenzen, C.J.; Holmes, R.W.; Strickland, J.D.H. Fluorometric Determination of Chlorophyll. *ICES J. Mar. Sci.* **1965**, *30*, 3–15. [[CrossRef](#)]
46. Vidussi, F.; Claustre, H.; Bustillos-Guzmán, J.; Cailliau, C.; Marty, J.-C. Determination of chlorophylls and carotenoids of marine phytoplankton: Separation of chlorophyll *a* from divinylchlorophyll *a* and zeaxanthin from lutein. *J. Plankton Res.* **1996**, *18*, 2377–2382. [[CrossRef](#)]
47. Brunet, C.; Mangoni, O. Determinazione quali-quantitativa dei pigmenti fitoplanctonici mediante HPLC. In *Metodologie di Studio del Plancton Marino*; Manuali e Linee Guida 56/2010; Socal, G., Buttino, I., Cabrini, M., Mangoni, O., Penna, A., Totti, C., Eds.; ISPRA: Roma, Italy, 2010; pp. 379–385. ISBN 978-88-448-0427-5.
48. DiTullio, G.R.; Geesey, M.E.; Leventer, A.; Lizotte, M.P. Algal pigment ratios in the Ross Sea: Implications for Chemtax analysis of Southern Ocean data. In *Antarctic Research Series*; DiTullio, G.R., Dunbar, R.B., Eds.; American Geophysical Union: Washington, DC, USA, 2003; Volume 78, pp. 35–51. ISBN 978-0-87590-972-1.
49. DiTullio, G.R.; Garcia, N.; Riseman, S.F.; Sedwick, P.N. Effects of iron concentration on pigment composition in *Phaeocystis antarctica* grown at low irradiance. *Biogeochemistry* **2007**, *83*, 71–81. [[CrossRef](#)]
50. van Leeuwe, M.A.; Visser, R.J.W.; Stefels, J. The pigment composition of *Phaeocystis antarctica* (Haptophyceae) under various conditions of light, temperature, salinity, and iron. *J. Phycol.* **2014**, *50*, 1070–1080. [[CrossRef](#)]
51. Mangoni, O.; Saggiomo, M.; Bolinesi, F.; Castellano, M.; Povero, P.; Saggiomo, V.; DiTullio, G.R. *Phaeocystis antarctica* unusual summer bloom in stratified Antarctic coastal waters (Terra Nova Bay, Ross Sea). *Mar. Environ. Res.* **2019**, *151*, 104733. [[CrossRef](#)]
52. Demers, S.; Roy, S.; Gagnon, R.; Vignault, C. Rapid light-induced changes in cell fluorescence and in xanthophyll-cycle pigments of *Alexandrium excavatum* (Dinophyceae) and *Thalassiosira pseudonana* (Bacillariophyceae): A photo-protection mechanism. *Mar. Ecol. Prog. Ser.* **1991**, *76*, 185–193. [[CrossRef](#)]
53. Meyer, A.A.; Tackx, M.; Daro, N. Xanthophyll cycling in *Phaeocystis globosa* and *Thalassiosira* sp.: A possible mechanism for species succession. *J. Sea Res.* **2000**, *43*, 373–384. [[CrossRef](#)]
54. Mangoni, O.; Carrada, G.C.; Modigh, M.; Catalano, G.; Saggiomo, V. Photoacclimation in Antarctic bottom ice algae: An experimental approach. *Polar Biol.* **2009**, *32*, 325–335. [[CrossRef](#)]
55. Mauzerall, D.; Greenbaum, N.L. The absolute size of a photosynthetic unit. *Biochim. Biophys. Acta BBA—Bioenerg.* **1989**, *974*, 119–140. [[CrossRef](#)]
56. Falkowski, P.G.; Raven, J.A. *Aquatic Photosynthesis*; Blackwell Science: Malden, MA, USA, 1997; ISBN 978-0-86542-387-9.
57. Cullen, J.J.; Davis, R.F. The blank can make a big difference in oceanographic measurements. *Limnol. Oceanogr. Bull.* **2003**, *12*, 29–35. [[CrossRef](#)]
58. Maxwell, K.; Johnson, G.N. Chlorophyll fluorescence—A practical guide. *J. Exp. Bot.* **2000**, *51*, 659–668. [[CrossRef](#)] [[PubMed](#)]
59. Schreiber, U.; Klughammer, C.; Kolbowski, J. Assessment of wavelength-dependent parameters of photosynthetic electron transport with a new type of multi-color PAM chlorophyll fluorometer. *Photosynth. Res.* **2012**, *113*, 127–144. [[CrossRef](#)] [[PubMed](#)]
60. Arrigo, K.R.; DiTullio, G.R.; Dunbar, R.B.; Robinson, D.H.; VanWoert, M.; Worthen, D.L.; Lizotte, M.P. Phytoplankton taxonomic variability in nutrient utilization and primary production in the Ross Sea. *J. Geophys. Res. Oceans* **2000**, *105*, 8827–8846. [[CrossRef](#)]

61. Bertrand, E.M.; Saito, M.A.; Lee, P.A.; Dunbar, R.B.; Sedwick, P.N.; DiTullio, G.R. Iron Limitation of a Springtime Bacterial and Phytoplankton Community in the Ross Sea: Implications for Vitamin B₁₂ Nutrition. *Front. Microbiol.* **2011**, *2*. [[CrossRef](#)]
62. Ryan-Keogh, T.J.; DeLizo, L.M.; Smith, W.O.; Sedwick, P.N.; McGillicuddy, D.J.; Moore, C.M.; Bibby, T.S. Temporal progression of photosynthetic-strategy in phytoplankton in the Ross Sea, Antarctica. *J. Mar. Syst.* **2017**, *166*, 87–96. [[CrossRef](#)]
63. van Boekel, W.H.M. Phaeocystis colony mucus components and the importance of calcium ions for colony stability. *Mar. Ecol.-Prog. Ser.* **1992**, *87*, 301–305. [[CrossRef](#)]
64. Smith, W.O.; Dinniman, M.S.; Klinck, J.M.; Hofmann, E. Biogeochemical climatologies in the Ross Sea, Antarctica: Seasonal patterns of nutrients and biomass. *Deep Sea Res. Part II Top. Stud. Oceanogr.* **2003**, *50*, 3083–3101. [[CrossRef](#)]
65. Tang, K.W.; Smith, W.O., Jr.; Elliott, D.T.; Shields, A.R. Colony size of *Phaeocystis antarctica* (Prymnesiophyceae) as influenced by zooplankton grazers. *J. Phycol.* **2008**, *44*, 1372–1378. [[CrossRef](#)]
66. Lohr, M.; Wilhelm, C. Xanthophyll synthesis in diatoms: Quantification of putative intermediates and comparison of pigment conversion kinetics with rate constants derived from a model. *Planta* **2001**, *212*, 382–391. [[CrossRef](#)]
67. Thingstad, F.; Billen, G. Microbial degradation of *Phaeocystis* material in the water column. *J. Mar. Syst.* **1994**, *5*, 55–65. [[CrossRef](#)]
68. Solomon, C.M.; Lessard, E.J.; Keil, R.G.; Foy, M.S. Characterization of extracellular polymers of *Phaeocystis globosa* and *P. antarctica*. *Mar. Ecol. Prog. Ser.* **2003**, *250*, 81–89.
69. Lubbers, G.; Gieskes, W.; Castilho, P.; del Salomons, W.; Bril, J. Manganese accumulation in the high pH microenvironment of *Phaeocystis* sp. (Haptophyceae) colonies from the North Sea. *Mar. Ecol. Prog. Ser.* **1990**, *59*, 285–293. [[CrossRef](#)]
70. Smayda, T.J.; Reynolds, C.S. Strategies of marine dinoflagellate survival and some rules of assembly. *J. Sea Res.* **2003**, *49*, 95–106. [[CrossRef](#)]
71. Ross, O.; Sharples, J. Phytoplankton motility and the competition for nutrients in the thermocline. *Mar. Ecol. Prog. Ser.* **2007**, *347*, 21–38. [[CrossRef](#)]
72. Stoecker, D.K.; Hansen, P.J.; Caron, D.A.; Mitra, A. Mixotrophy in the Marine Plankton. *Annu. Rev. Mar. Sci.* **2017**, *9*, 311–335. [[CrossRef](#)]
73. Stamatakis, K.; Vayenos, D.; Kotakis, C.; Gast, R.J.; Papageorgiou, G.C. The extraordinary longevity of kleptoplasts derived from the Ross Sea haptophyte *Phaeocystis antarctica* within dinoflagellate host cells relates to the diminished role of the oxygen-evolving Photosystem II and to supplementary light harvesting by mycosporine-like amino acid/s. *Biochim. Biophys. Acta BBA—Bioenerg.* **2017**, *1858*, 189–195. [[CrossRef](#)]
74. Gast, R.J.; Fay, S.A.; Sanders, R.W. Mixotrophic Activity and Diversity of Antarctic Marine Protists in Austral Summer. *Front. Mar. Sci.* **2018**, *5*, 13. [[CrossRef](#)]
75. Bird, D.F.; Kalff, J. Bacterial Grazing by Planktonic Lake Algae. *Science* **1986**, *231*, 493–495. [[CrossRef](#)]
76. Nygaard, K.; Tobiesen, A. Bacterivory in algae: A survival strategy during nutrient limitation. *Limnol. Oceanogr.* **1993**, *38*, 273–279. [[CrossRef](#)]
77. Dolan, J.R.; Pérez, M.T. Costs, benefits and characteristics of mixotrophy in marine oligotrichs: Mixotrophy in marine oligotrichs. *Freshw. Biol.* **2000**, *45*, 227–238. [[CrossRef](#)]
78. Gast, R.J.; Moran, D.M.; Beaudoin, D.J.; Blythe, J.N.; Dennett, M.R.; Caron, D.A. Abundance of a novel Dinoflagellate phylotype in the Ross Sea, Antarctica. *J. Phycol.* **2006**, *42*, 233–242. [[CrossRef](#)]
79. Bolinesi, F.; Saggiomo, M.; Ardini, F.; Castagno, P.; Cordone, A.; Fusco, G.; Rivarolo, P.; Saggiomo, V.; Mangoni, O. Spatial-Related Community Structure and Dynamics in Phytoplankton of The Ross Sea, Antarctica. *Front. Mar. Sci.* submitted.
80. Deppeler, S.L.; Davidson, A.T. Southern Ocean Phytoplankton in a Changing Climate. *Front. Mar. Sci.* **2017**, *4*. [[CrossRef](#)]

